



Synthesis and biological evaluation of bivalent cannabinoid receptor ligands based on *hCB₂R* selective benzimidazoles reveal unexpected intrinsic properties

Martin Nimczick^{a,b}, Daniela Pemp^c, Fouad H. Darras^b, Xinyu Chen^{a,b}, Jörg Heilmann^c, Michael Decker^{a,c,*}

^a Pharmazeutische und Medizinische Chemie, Institut für Pharmazie und Lebensmittelchemie, Julius-Maximilians-Universität Würzburg, Am Hubland, D-97074 Würzburg, Germany

^b Lehrstuhl für Pharmazeutische Chemie I, Institut für Pharmazie, Universität Regensburg, Universitätsstraße 31, D-93053 Regensburg, Germany

^c Lehrstuhl für Pharmazeutische Biologie, Institut für Pharmazie, Universität Regensburg, Universitätsstraße 31, D-93053 Regensburg, Germany

ARTICLE INFO

Article history:

Received 24 March 2014

Revised 28 May 2014

Accepted 4 June 2014

Available online 13 June 2014

Keywords:

Bivalent ligand

Cannabinoid receptor

CB₂

Benzimidazole

ABSTRACT

The design of bivalent ligands targeting G protein-coupled receptors (GPCRs) often leads to the development of new, highly selective and potent compounds. To date, no bivalent ligands for the human cannabinoid receptor type 2 (*hCB₂R*) of the endocannabinoid system (ECS) are described. Therefore, two sets of homobivalent ligands containing as parent structure the *hCB₂R* selective agonist **13a** and coupled at different attachment positions were synthesized. Changes of the parent structure at these positions have a crucial effect on the potency and efficacy of the ligands. However, we discovered that bivalency has an influence on the effect at both cannabinoid receptors. Moreover, we found out that the spacer length and the attachment position altered the efficacy of the bivalent ligands at the receptors by turning agonists into antagonists and inverse agonists.

© 2014 Elsevier Ltd. All rights reserved.

1. Introduction

Since the identification of (–)-*trans*- Δ^9 -tetrahydrocannabinol as the major bioactive component in *Cannabis sativa* L. by Gaoni and Mechoulam in 1964,^{1,2} the biological system behind these physiological effects of natural cannabinoids was intensively studied. Moreover, the endocannabinoid system (ECS) was discovered, which consists of the endogenous ligands (endocannabinoids like anandamide or 2-arachidonoyl glycerol), the synthesis and deactivation of these ligands, the cannabinoid receptors and the intracellular signaling pathways activated by the endogenous ligands at the receptors. Till now, many ligands targeting the ECS were synthesized and two subtypes of cannabinoid receptors in humans were identified and characterized as G protein-coupled receptors

(GPCRs), the human cannabinoid receptor type 1 (*hCB₁R*) and human cannabinoid receptor type 2 (*hCB₂R*).^{3–6}

In the past decades, for many GPCRs bivalent ligands were designed, which consist of two ligands connected by a spacer. If both parent ligands (pharmacophores) are identical, then the bivalent ligand is called homobivalent, otherwise heterobivalent. For parent ligands, which are potent and selective to one GPCR subtype, and linked at a preferred position by an appropriate spacer with regards to chemical structure and length, it can be possible to achieve bivalent ligands with a high affinity for their receptor subtypes.^{7,8} If these bivalent ligands bridge two neighboring, orthosteric binding sites (i.e., the main binding site of the endogenous ligands) of two interacting GPCRs (homo- or heterodimers) or bind at orthosteric and allosteric binding sites (i.e., sites distinct from the orthosteric one, but able to influence binding of orthosteric ligands) of one GPCR, depends on the spacer structure and length, and this is often not clearly distinguishable.^{7–10}

However, so far it is possible to get bivalent ligands, which bind to a receptor subtype with a higher potency and selectivity than the original parent ligand or the corresponding univalent compound, which only consists of the pharmacophore connected with a spacer, for example, for the μ -opioid receptor^{11–14} or dopamine D₂ receptor.^{15–19} This suggests that bivalency can have a positive

Abbreviations: Ag, measuring in agonism mode; Ant, measuring in antagonism mode; atm., atmosphere; CDI, 1,1'-carbonyldiimidazole; DMF, *N,N*-dimethylformamide; DMSO, dimethyl sulfoxide; EC₅₀, half maximal effective concentration (potency); ECS, endocannabinoid system; E_{max}, maximal response (efficacy); GPCR, G protein-coupled receptor; GTPase, hydrolase for guanosine-5'-triphosphate; *hCB₁R*, human cannabinoid receptor type 1; *hCB₂R*, human cannabinoid receptor type 2; K_i, binding affinity; THF, tetrahydrofuran.

* Corresponding author. Tel.: +49 931 31 89676; fax: +49 931 31 85494.

E-mail address: michael.decker@uni-wuerzburg.de (M. Decker).

effect on the binding properties and furthermore can lead to new options in the research and study of receptor subtypes, but also in the development of new drugs, for example, hexoprenaline (a bivalent norepinephrine coupled with a hexane spacer) as a selective β_2 adrenergic receptor agonist applied in the treatment of asthma (Fig. 1).^{20,21}

For the cannabinoid receptors the first ‘bivalent’ cannabinoids were synthesized by connecting cannabinoids with an ethane bridge in 1981.²² Afterwards, the next bivalent ligands were selective for the hCB_1R by linking of the known, selective hCB_1R inverse agonist drug rimonabant at the carboxamide with different spacers instead of piperidine (Fig. 1).^{23,24} Hereby, a suitable spacer structure consisted of two hydrophobic alkylene chains at a secondary or tertiary amine. Their optimal spacer length for the highest receptor affinity was 15 atoms.²³ Moreover, heterobivalent ligands targeting the CB_1R and μ -opioid receptor were developed by coupling of modified rimonabant with the known, selective μ -opioid receptor agonist α -oxymorphone.²⁵ But, no bivalent ligands for the CB_2R have been reported to date.

Therefore, we designed bivalent ligands for the hCB_2R . An appropriate hCB_2 ligand may be the highly selective and potent hCB_2R agonist **13a**, which was developed by AstraZeneca and published in 2008 (Fig. 2).²⁶ Assumed attachment positions were the *para*-ethoxy group of the benzyl substituent in position 2, the *N*-alkyl substituent in position 1 and the amide at the carboxyl group in position 5 of the benzimidazole (shown in Fig. 2). At these positions, it is feasible to introduce a spacer by the synthetic way without significant changes at the ligand's chemical structure.

The *para*-ethoxy group is a determining factor for the efficacy of the pharmacophore as an agonist²⁷ and therefore this position is not a suitable connection position to evaluate the effect of bivalency on ligand binding. At the nitrogen of the imidazole branched, cyclic or aromatic substituents were introduced. Beside these hydrophobic side chains, ligands with basic substituents had also been synthesized.²⁶ In order to prove that a linear substituent can be tolerated there and consequently this position is suited for linear spacers, a modified ligand **13b** with a linear alkyl chain at the imidazole was synthesized and tested. Then the parent structure was coupled at the imidazole with different spacers to achieve a set of bivalent and univalent ligands (**17a–b**, **21a–c**). On position 5 of the benzimidazole, different carboxamides with linear and large hydrophobic amines have been synthesized already.²⁶ In addition, other functional groups like amido, ido, sulfonamido or sulfonyl had been introduced.^{26,28–31} Therefore, we presumed that the amide is also an appropriate position to link the parent ligand. It was connected with different spacers at the

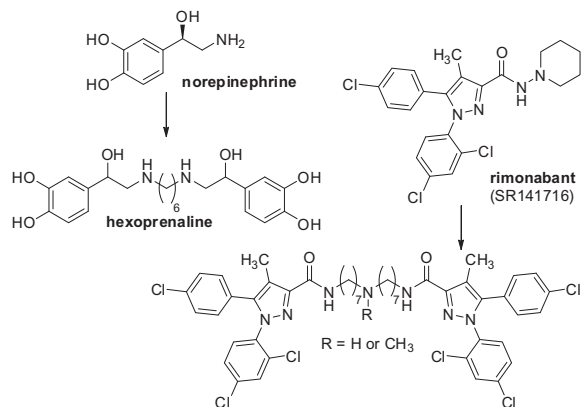


Figure 1. Examples of bivalent ligands: hexoprenaline (bivalent norepinephrine) as a β_2 adrenergic receptor agonist^{20,21} and bivalent, potent hCB_1R inverse agonists²³ constructed from rimonabant.

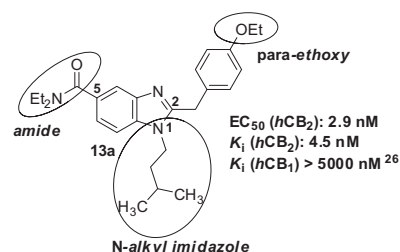


Figure 2. Structure of the selective hCB_2R agonist **13a**²⁶ and possible connecting positions (ellipses, italic).

amide to achieve a second set of bivalent and univalent ligands (**26a–b**, **31a–b**). We presumed that these bivalent compounds for both attachment positions can selectively target the hCB_2R and may be new pharmacological probes to investigate this receptor subtype. Additionally, the methyl ester at position 5 of the benzimidazole (**13c**) was synthesized to find out, whether the ester function is tolerated, and thus bivalent ligands with an ester coupling might be promising.¹²

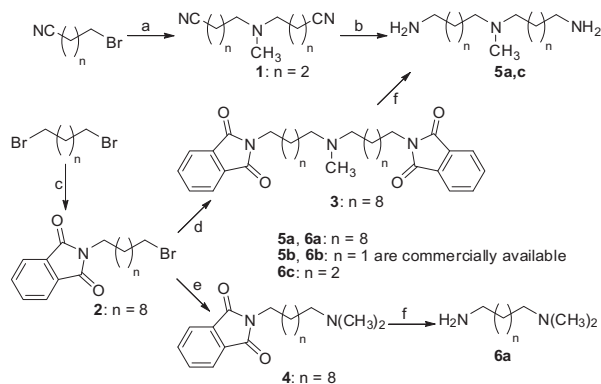
Short (7–9 atoms) and long (21 atoms) spacers were utilized to investigate the influence of spacer length on potency and efficacy. These spacers had the same structure as the suitable spacers for bivalent, hCB_1R selective inverse agonists with a tertiary amine.²³ The symmetric, bivalent spacers consists of two alkylene chains combined through methylamine. For the univalent spacers we used the ‘half’ bivalent spacers, the alkylene chain is linked to dimethylamine. We consider these univalent ligands were necessary to study the influence of bivalency on the effect of the ligands at the receptors and to distinguish this effect of bivalent from the univalent ones, which we assumed to differ from the parent ligand.

The potency and efficacy of all compounds at the hCB_2R and hCB_1R were determined in a functional steady-state GTPase assay as previously described.^{32–34}

2. Results and discussion

2.1. Chemistry

The spacers were synthesized via two strategies (Scheme 1): The first possibility is the substitution of the bromide from an ω -bromoalkylnitrile with methylamine to get the corresponding tertiary amine **1**. The cyano groups were then reduced by tetrahydrofuran-borane to the primary amines of the bivalent spacer **5a,c**.



Scheme 1. Synthesis of spacer structures. Reagents and conditions: (a) $H_2NCH_3 \cdot HCl$, K_2CO_3 , KI , CH_3CN , 18 h, reflux, N_2 atm.; (b) $BH_3 \cdot THF$, THF , 2 h, reflux; (c) potassium phthalimide, DMF , 7 d, rt; (d) $H_2NCH_3 \cdot HCl$, K_2CO_3 , CH_3CN , 18 h, 50 °C, N_2 atm.; (e) $HN(CH_3)_2 \cdot HCl$, K_2CO_3 , CH_3CN , 18 h, 50 °C, N_2 atm.; (f) $H_2NNH_2 \cdot H_2O$, C_2H_5OH , 18 h, 50 °C, N_2 atm.

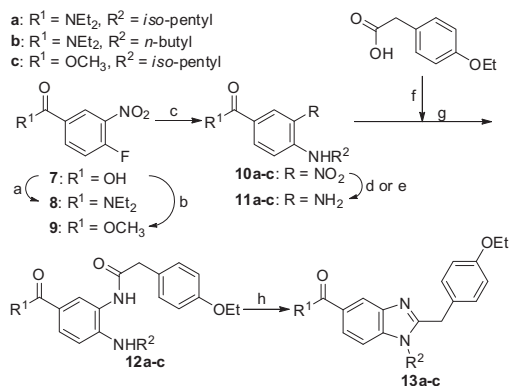
For longer spacers, the ω -bromoalkyl nitrile has to be synthesized by a reaction of α,ω -dibromoalkane with sodium cyanide. For spacers with ten carbon atoms on each side, however, the following coupling with methylamine did not yield the desired product. Therefore, these longer spacers were synthesized through a second strategy: At first, an α,ω -dibromoalkane and potassium phthalimide formed the corresponding *N*- ω -bromoalkylphthalimide **2**. It was reacted with dimethylamine or methylamine to the corresponding bivalent (**3**) and univalent (**4**) spacers 'protected' by phthalimide, respectively. In this Gabriel synthesis, the bivalent spacer **5a** and the univalent spacer **6a** were finally obtained by hydrazinolysis.

All ligands were synthesized following a general procedure. The synthesis of the parent structures without a spacer, including the reference ligand **13a**,²⁶ is shown in Scheme 2.

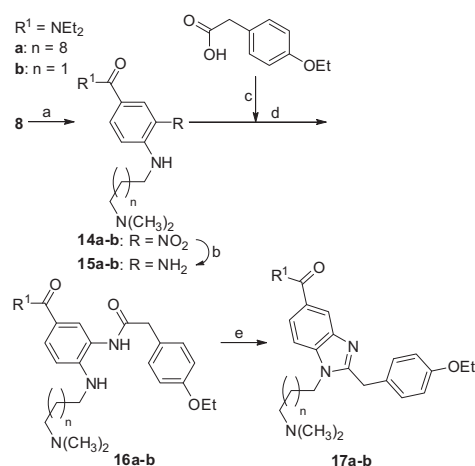
Firstly, the carboxyl group of 4-fluoro-3-nitrobenzoic acid **7** was activated by oxalyl dichloride and connected with diethyl amine to get the corresponding amide **8**. The formation of the methyl ester **9** was achieved under reflux conditions in methanol with a catalytic amount of sulfuric acid. Secondly, compounds **10a–c** were prepared by substitution of the fluoride with the corresponding primary amines. Then the nitro group was reduced by stannous chloride dihydrate or under acidic conditions using iron powder to the corresponding 3,4-diaminophenyl compounds **11a–c**. The color of all 3,4-diaminophenyl compounds becomes darker over time. This suggests that these structures are susceptible to oxidation or in another way instable. Due to the instability of the intermediates, the reduction and also the following amidation were carried out under argon or nitrogen atmosphere, and the 3,4-diaminophenyl compounds were immediately used in the next step. They were coupled with 4-ethoxyphenylacetic acid, which was first activated by CDI, to get the corresponding amides **12a–c**. Finally, the benzimidazoles **13a–c** were obtained by condensation and ring-closure in glacial acetic acid.

For preparation of uni- and bivalent ligands, this general procedure was slightly modified. To form univalent ligands **17a–b** (Scheme 3) and bivalent ligands **21a–c** (Scheme 4), the connection at the imidazole was achieved by substitution of the fluoride in the second step with the primary amines of the spacers.

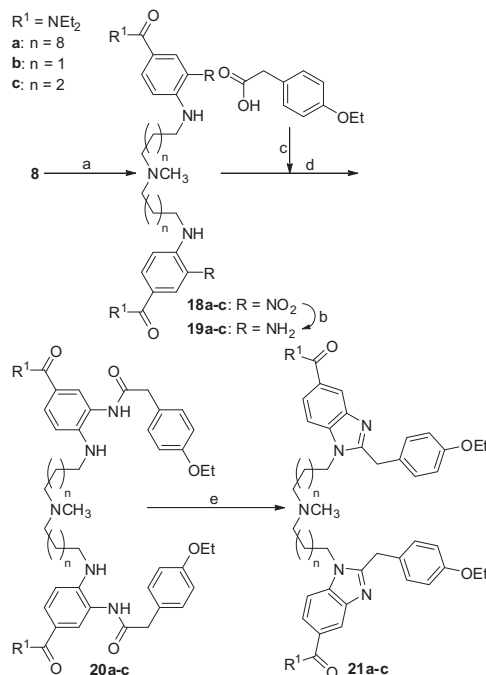
To obtain univalent ligands **26a–b** (Scheme 5) and bivalent ligands **31a–b** (Scheme 6), the connection at the amide was achieved by amidation of the carboxyl group in the first step of the general procedure with the primary amines of the spacers.



Scheme 2. Synthesis of parent structures **13a–c**. Reagents and conditions: (a) i. $(\text{COCl})_2$, DMF, CH_2Cl_2 , 2 h, rt, ii. $\text{HN}(\text{C}_2\text{H}_5)_2$, $\text{N}(\text{C}_2\text{H}_5)_3$, CH_2Cl_2 , 18 h, rt; (b) CH_3OH , H_2SO_4 , 2 d, reflux; (c) H_2NR^2 , $\text{N}(\text{C}_2\text{H}_5)_3$, $\text{C}_2\text{H}_5\text{OH}$, 18 h, 50–75 °C; (d) for **11a–b**: $\text{SnCl}_2 \cdot 2\text{H}_2\text{O}$, $\text{C}_2\text{H}_5\text{OH}$, 18 h, 75 °C, Ar atm.; (e) for **11c**: Fe powder, HCl, $\text{C}_2\text{H}_5\text{OH}/\text{H}_2\text{O}$ 4:1, 2 h, reflux, Ar atm.; (f) CDI, dry THF, 2 h, rt; (g) dry THF, 18 h, 50 °C, Ar atm.; (h) glacial CH_3COOH , 1.5–3 h, reflux.



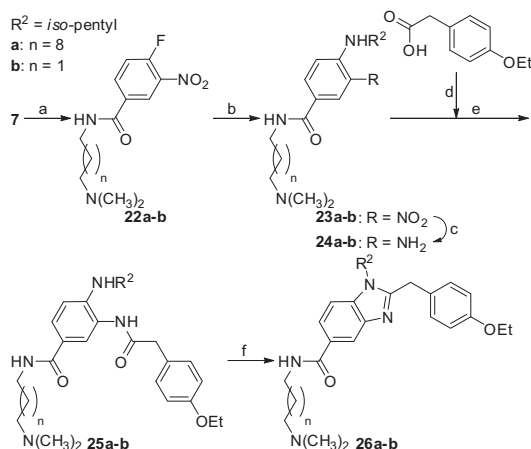
Scheme 3. Synthesis of univalent ligands **17a–b**. Reagents and conditions: (a) **6a–b**, $\text{N}(\text{C}_2\text{H}_5)_3$, $\text{C}_2\text{H}_5\text{OH}$, 18 h, 50–75 °C; (b) Fe powder, HCl, $\text{C}_2\text{H}_5\text{OH}/\text{H}_2\text{O}$ 4:1, 2 h, reflux, Ar/ N_2 atm.; (c) CDI, dry THF, 2 h, rt; (d) dry THF, 18 h, 50 °C, Ar/ N_2 atm.; (e) glacial CH_3COOH , 1.5–3 h, reflux.



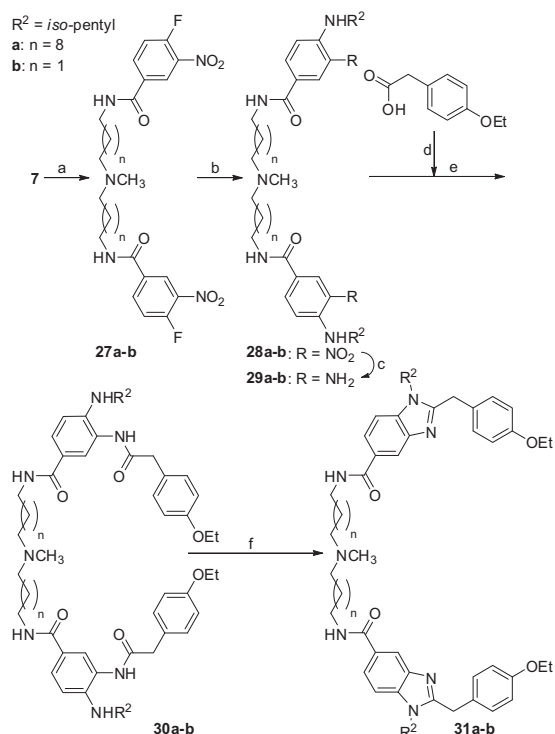
Scheme 4. Synthesis of bivalent ligands **21a–c**. Reagents and conditions: (a) **5a–c**, $\text{N}(\text{C}_2\text{H}_5)_3$, $\text{C}_2\text{H}_5\text{OH}$, 18 h, 50–75 °C; (b) $\text{SnCl}_2 \cdot 2\text{H}_2\text{O}$, $\text{C}_2\text{H}_5\text{OH}$, 18 h, 75 °C, Ar atm.; (c) CDI, dry THF, 2 h, rt; (d) dry THF, 18 h, 50 °C, Ar atm.; (e) glacial CH_3COOH , 1.5–3 h, reflux.

2.2. Functional steady-state GTPase assay

For the functional steady-state GTPase assay, the membrane of Sf9 cells expressing *hCB₂R-G α_{i2}* or *hCB₁R-G α_{i2}* fusion protein together with $\text{G}\beta_1\gamma_2$ and RGS4 was used. Activation of the receptors by an agonist leads to an exchange of GDP against GTP at the $\text{G}\alpha$ -subunit of the heterotrimeric G protein. Once GTP is bound, the ternary G protein complex dissociates into the $\text{G}\alpha$ -GTP- and the $\text{G}\beta\gamma$ -subunit. The $\text{G}\alpha$ -subunit itself functions as a GTPase and catalyzes the hydrolysis of bound GTP to bound GDP and free inorganic phosphate (P_i). This deactivates the G protein by forming the $\text{G}\alpha$ -GDP-subunit and subsequent reorganizing the G protein. Using $[\gamma\text{-}^{33}\text{P}]\text{GTP}$, the GTPase activity of the $\text{G}\alpha$ -subunit can be calculated



Scheme 5. Synthesis of univalent ligands **26a–b**. Reagents and conditions: (a) i. $(\text{COCl})_2$, DMF, CH_2Cl_2 , 2 h, rt, ii. **6a–b**, $\text{N}(\text{C}_2\text{H}_5)_3$, CH_2Cl_2 , 18 h, rt; (b) isopentylamine, $\text{N}(\text{C}_2\text{H}_5)_3$, $\text{C}_2\text{H}_5\text{OH}$, 18 h, 50–75 °C; (c) Fe powder, HCl, $\text{C}_2\text{H}_5\text{OH}/\text{H}_2\text{O}$ 4:1, 2 h, reflux, Ar/N_2 atm.; (d) CDI, dry THF, 2 h, rt; (e) dry THF, 18 h, 50 °C, Ar/N_2 atm.; (f) glacial CH_3COOH , 1.5–3 h, reflux.



Scheme 6. Synthesis of bivalent ligands **31a–b**. Reagents and conditions: (a) i. $(\text{COCl})_2$, DMF, CH_2Cl_2 , 2 h, rt, ii. **5a–b**, $\text{N}(\text{C}_2\text{H}_5)_3$, CH_2Cl_2 , 18 h, rt; (b) isopentylamine, $\text{N}(\text{C}_2\text{H}_5)_3$, $\text{C}_2\text{H}_5\text{OH}$, 18 h, 50–75 °C; (c) $\text{SnCl}_2 \cdot 2\text{H}_2\text{O}$, $\text{C}_2\text{H}_5\text{OH}$, 18 h, 75 °C, Ar atm.; (d) CDI, dry THF, 2 h, rt; (e) dry THF, 18 h, 50 °C, Ar atm.; (f) glacial CH_3COOH , 1.5–3 h, reflux.

by determining the amount of free $^{33}\text{P}_i$ and be used as a functional parameter for $h\text{CB}_2\text{R}$ or $h\text{CB}_1\text{R}$ activation.^{34,35}

In the steady-state GTPase assay the efficacy of all compounds was determined by screening a high concentration in agonism mode (Ag, without additional CP 55,940) and in antagonism mode (Ant, in presence of 30 nM CP 55,940) at the $h\text{CB}_2\text{R}$ and $h\text{CB}_1\text{R}$. The agonistic or inverse agonistic effect of a ligand can be determined directly in Ag. After a prestimulation of the receptors by a low concentration of the agonist CP 55,940, the inhibition of their response

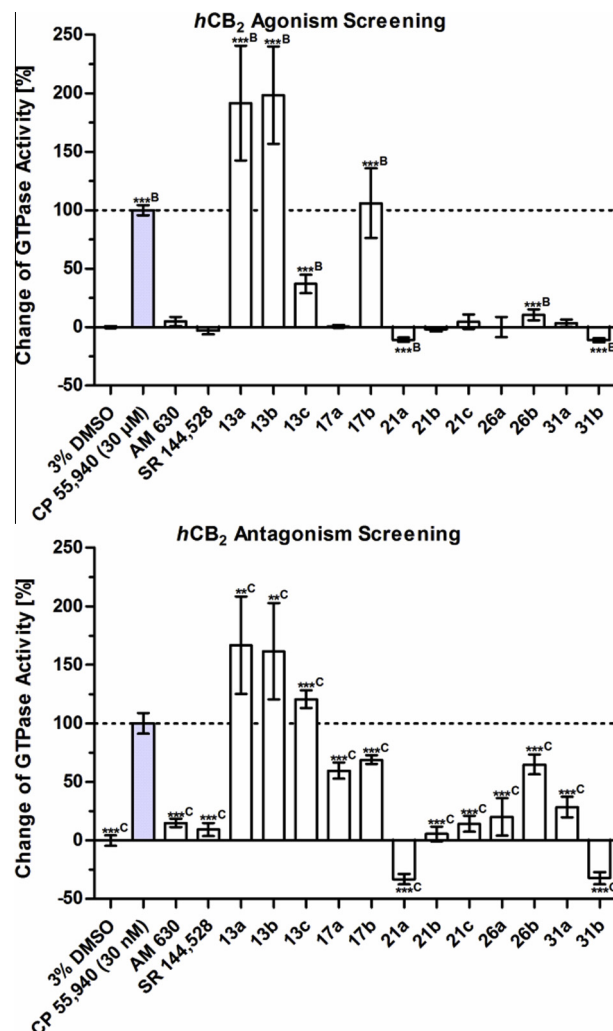


Figure 3. Functional steady-state GTPase assay results (mean \pm SD) at the $h\text{CB}_2\text{R}$ in agonism mode (applying a 30 μM concentration) and antagonism mode (applying a 30 μM concentration in presence of 30 nM CP 55,940), respectively. Significant differences: ** ($p < 0.01$), *** ($p < 0.001$), B: compared to basal GTPase activity (3% DMSO), C: compared to CP 55,940.

by antagonists (or inverse agonists) can be measured. The results are represented for $h\text{CB}_2\text{R}$ in Figure 3, for $h\text{CB}_1\text{R}$ in Figure 4.

According to these results, the potency of the compounds to each receptor was determined as a dose–response curve of different concentrations in the appropriate mode. Thus, the EC_{50} values of agonists were measured in Ag and refer to their agonistic effect of increasing concentrations. In Ant the EC_{50} values of antagonists and inverse agonists (* in Table 1) were determined after a prestimulation of the receptors by CP 55,940 and refer to the inhibition of the agonistic effect with increasing concentrations. The results are summarized in Table 1.

The reference compound and parent ligand **13a** shows a significantly higher agonistic effect at the $h\text{CB}_2\text{R}$ as CP 55,940, and also a similar submicromolar potency like this standard agonist. Therefore, compound **13a** is as described a high efficient and potent agonist at the $h\text{CB}_2\text{R}$. In our functional assay conditions the ligand **13a** showed a 49-fold lower potency in the submicromolar range than the reference value in GTP γS and radioligand binding assays.²⁶ The difference in potency of ligands had already been observed in previous studies for the standard compounds CP 55,940 and AM 251 as the functional steady-state GTPase assay determined lower affinities than the literature values.³² This can be explained

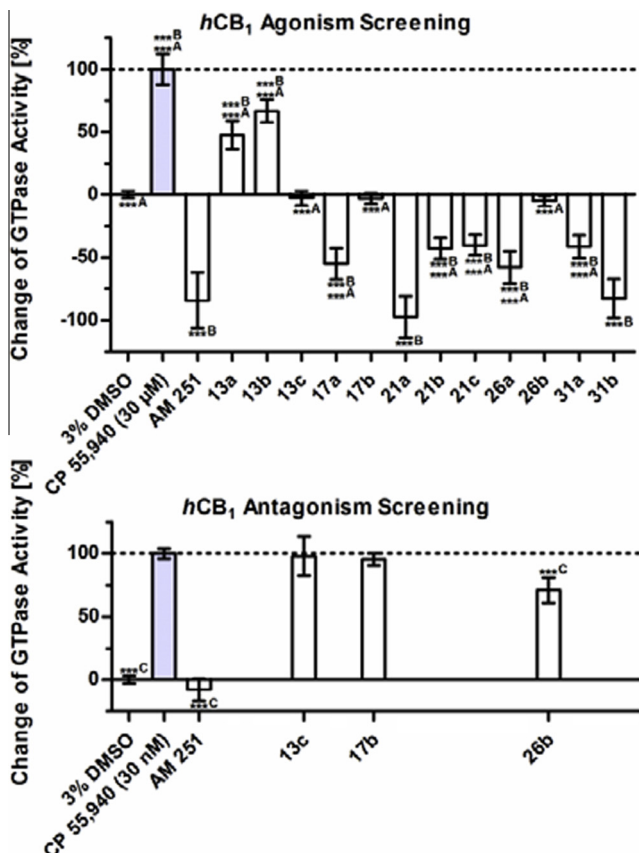


Figure 4. Functional steady-state GTPase assay results (mean \pm SD) at the *hCB₁*R in agonism mode (applying a 30 μ M concentration) and antagonism mode (only standard compounds and inactive compounds according to the results in agonism mode; applying a 30 μ M concentration in presence of 30 nM CP 55,940), respectively. Significant differences: *** ($p < 0.001$), A: compared to AM 251, B: compared to basal GTPase activity (3% DMSO), C: compared to CP 55,940.

by the different assay conditions (human cells, radioligand versus Sf9 cells, GTPase measurements), but also by the concept of ligand specific receptor conformation as in the functional assay a *hCB₁*-G α_{12} fusion system co-expressing G $\beta_1\gamma_2$ and RGS4 was used.³³ Therefore, for the results obtained for uni- and bivalent compounds in this assay it is reasonable to assume higher affinities in radioligand binding studies.

The modified ligand **13b** with a linear *n*-butyl side chain at the imidazole instead of the branched isopentyl substituent has a similar agonistic effect and potency at the *hCB₂*R like the parent ligand **13a**. Therefore, branched, cyclic or aromatic side chains at the imidazole are not essential for high efficient and potent *hCB₂*R agonists. Moreover, compound **13b** shows similar properties at the *hCB₁*R like the known *hCB₂*R-selective agonist **13a**. These higher EC₅₀ values of both ligands at the *hCB₁*R (23-fold for **13a**, 8-fold for **13b**) exhibit selectivity to the *hCB₂*R.

The methyl ester **13c** shows agonism at the *hCB₂*R in the submicromolar range, too. In contrast to the ligands **13a** and **13b**, it is totally inactive at the *hCB₁*R. This demonstrates that compound **13c** has a higher selectivity to the *hCB₂*R than the parent structure **13a**. Thus, the ester function at position 5 of the benzimidazole is tolerated and bivalent ligands with an ester coupling might theoretically be possible. The development of ester-based bivalent ligands can be possible despite metabolic lability of ester bonds, for example, when suitable sterically hindered dicarboxylic acids are applied as spacers, as shown for bivalent opioid-ligands.¹²

For univalent ligands **17a–b** and bivalent ligands **21a–c**, which are coupled with the spacer at the imidazole of the parent

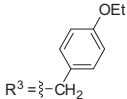
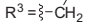
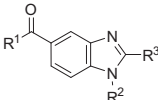
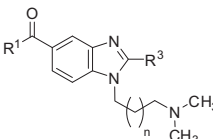
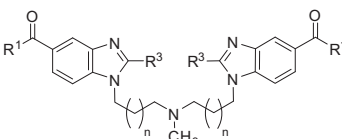
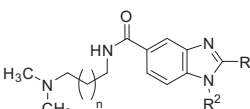
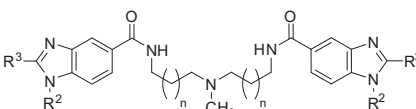
structure, the effect at the *hCB₂*R changes dramatically. Only the univalent compound **17b** with a short spacer activates the receptor, as well as it reduces the effect of the agonist CP 55,940 and therefore constitutes a partial agonist. The potency decreases to the micromolar range at the *hCB₂*R and exhibits total inactivity at the *hCB₁*R. This shows that ligand **17b** still has selectivity to the *hCB₂*R. The corresponding bivalent ligand **21b** shows antagonism at the *hCB₂*R with a similar micromolar potency like compound **17b**. Therefore, for this short spacer at the imidazole, bivalency changes the efficacy from partial agonism to antagonism, but not their potency. Also the bivalent compound **21c** with a slightly longer spacer is a micromolar antagonist like ligand **21b**. At the *hCB₁*R, bivalency shifts the effect from agonism of the parent structures **13a–b** to a significant inverse agonism of the bivalent ligands **21b–c** (the univalent compound **17b** was inactive). Their inverse agonism is only moderate compared to the standard inverse agonist AM 251. Moreover, the potency of both bivalent compounds decreases to the micromolar or higher range at the *hCB₁*R. Thus, selectivity over the *hCB₂*R is lost due to bivalency.

For univalent ligand **17a** and bivalent ligand **21a** with a long spacer at the imidazole, the effects at the receptors also change drastically. The univalent compound **17a** is an antagonist at the *hCB₂*R. For the corresponding bivalent compound **21a** it changes to a significant, inverse agonism at the *hCB₂*R, which is larger than the slightly negative effect of the standard inverse agonist SR 144,528. At the *hCB₁*R, both compounds are inverse agonists. Univalent ligand **17a** shows a less pronounced inverse agonism than corresponding bivalent ligand **21a**, which is a similar full inverse agonist like AM 251. The potency of both compounds with long spacer decreases to the micromolar range at both receptors and thus they lose selectivity, too. However, bivalency has also an effect by changing the efficacy from antagonism to inverse agonism at the *hCB₂*R or an increase of the inverse agonism at the *hCB₁*R.

For univalent ligands **26a–b** and bivalent ligands **31a–b**, which are connected at the amide with the spacer, the effects at the receptors also change dramatically, but in a different way. Compared to the parent ligand **13a**, the efficacy is changed, the potency decreases to the micromolar or higher range at both receptors and thus they are no more selective to the *hCB₂*R. The univalent compound **26b** with a short spacer is less potent at both receptors. The corresponding bivalent compound **31b** still shows an unselective, micromolar activity. Thus, in this case the bivalency is able to increase the potency at both receptors. The univalent ligand **26b** has a weak agonism at the *hCB₂*R and reduces the effect of CP 55,940. So, compared to the univalent ligand **17b** with this short spacer at the imidazole, this compound **26b** is a partial agonist, too. The corresponding bivalent ligand **31b** shows a significant, inverse agonism at the *hCB₂*R, which is higher than the slightly negative effect of SR 144,528. Instead of antagonism like for bivalent ligand **21b** with the short spacer at the imidazole, the bivalent ligand **31b** with this spacer at the amide is now an inverse agonist. Therefore, the connecting position has also an influence on efficacy beside the bivalency. At the *hCB₁*R, compound **26b** is an antagonist with a slight decrease of the effect of CP 55,940. The corresponding bivalent compound **31b** shows full inverse agonism at the *hCB₁*R on the same level as AM 251. Altogether, for this short spacer at the amide the bivalency changes the efficacy to inverse agonism and increases the potency at both receptors.

Univalent ligand **26a** and corresponding bivalent ligand **31a** with a long spacer are antagonists at the *hCB₂*R and moderate inverse agonists at the *hCB₁*R. Therefore, for this long spacer at the amide, bivalency has no influence on potency or efficacy at both receptors. However, the connecting position of the bivalent compounds has an influence on efficacy at the *hCB₂*R. Instead of inverse agonism like the bivalent compound **21a** with the long

Table 1
Results of the functional steady-state GTPase assayⁱ

Structures	Compound	hCB ₂ R				hCB ₁ R			
		E_{\max}^a (%) Ag	E_{\max}^b (%) Ant	LogEC ₅₀ ^c	EC ₅₀ ^c	E_{\max}^a (%) Ag	E_{\max}^b (%) Ant	LogEC ₅₀ ^d	EC ₅₀ ^d
	3% DMSO ^f	0 ± 1	0 ± 5			0 ± 3	0 ± 3		
 R ³ =  -CH ₂	CP 55,940 ^{g,h}	100 ± 4	100 ± 9	-7.39 ± 0.12	40.7 nM	100 ± 12	100 ± 4	-7.89 ± 0.15	12.9 nM
	AM 630 ^g	5 ± 4	15 ± 3	-6.22 ± 0.20*	603 nM*				
	SR 144,528 ^g	-3 ± 3	9 ± 6	-6.13 ± 0.53*	741 nM*				
	AM 251 ^h					-84 ± 22	-8 ± 9	-7.24 ± 0.15*	57.5 nM*
 R ¹ = NEt ₂ ; R ² = <i>iso</i> -pentyl R ¹ = NEt ₂ ; R ² = <i>n</i> -butyl R ¹ = OCH ₃ ; R ² = <i>iso</i> -pentyl	13a	192 ± 49	167 ± 42	-6.85 ± 0.38 Lit.: 2.9 nM; K _i = 4.5 nM ^g	141 nM	48 ± 11		-5.49 ± 0.44 Lit.: K _i > 5000 nM ^g	3.24 μM
	13b	198 ± 42	162 ± 41	-6.76 ± 0.40	174 nM	67 ± 9		-5.87 ± 0.36	1.35 μM
	13c	37 ± 8	121 ± 7	-6.53 ± 0.09	295 nM	-3 ± 6	98 ± 15	NT	
 R ¹ = NEt ₂ ; <i>n</i> = 8 R ¹ = NEt ₂ ; <i>n</i> = 1	17a	1 ± 1	60 ± 7	-4.50 ± 0.34*	31.6 μM*	-55 ± 12		-4.60 ± 0.18*	25.1 μM*
	17b	106 ± 30	69 ± 4	-4.90 ± 0.25	12.6 μM	-3 ± 4	95 ± 5	NT	
 R ¹ = NEt ₂ ; <i>n</i> = 8 R ¹ = NEt ₂ ; <i>n</i> = 1 R ¹ = NEt ₂ ; <i>n</i> = 2	21a	-11 ± 2	-33 ± 4	-5.18 ± 0.18*	6.61 μM*	-97 ± 17		-5.20 ± 0.17*	6.31 μM*
	21b	-2 ± 2	5 ± 6	-4.92 ± 0.11*	12.0 μM*	-43 ± 8		-4.46 ± 0.64*	34.7 μM*
	21c	5 ± 6	14 ± 7	-4.24 ± 0.18*	57.5 μM*	-40 ± 8		ND*	>100 μM*
 R ² = <i>iso</i> -pentyl; <i>n</i> = 8 R ² = <i>iso</i> -pentyl; <i>n</i> = 1	26a	0 ± 9	20 ± 16	-4.71 ± 0.29*	19.5 μM*	-58 ± 13		-4.62 ± 0.15*	24.0 μM*
	26b	11 ± 5	65 ± 9	ND*	>100 μM*	-5 ± 4	71 ± 10	ND*	>100 μM*
 R ² = <i>iso</i> -pentyl; <i>n</i> = 8 R ² = <i>iso</i> -pentyl; <i>n</i> = 1	31a	3 ± 3	28 ± 9	-4.78 ± 0.11*	16.6 μM*	-42 ± 9		-4.59 ± 0.49*	25.7 μM*
	31b	-11 ± 2	-32 ± 5	-5.54 ± 0.24*	2.88 μM*	-83 ± 16		-4.76 ± 0.30*	17.4 μM*

^a Screening in Ag (without additional CP 55,940).

^b Screening in *Ant* (in presence of 30 nM CP 55,940).

^c Values with * in *Ant*; CP 55,940, **13a–c** and **17b** in *Ag*.

^d Values with * in *Ant*; CP 55,940 and **13a-b** in *Ag*.

^e Reference values: EC₅₀ value from a functional GTPγS assay, K_i values from a radioligand binding assay.²⁶

^f Basal GTPase activity.

^g Standard compounds for *hCB₂R*: agonist CP 55,940, antagonist AM 630, inverse agonist SR 144,528.^{3,36–38}

^h Standard compounds for *hCB₁R*: agonist CP 55,940, inverse agonist AM 251. ^{3,38,39}

standard compounds for nCB1R: agonist CI 55,940, inverse agonist AM 251.

¹ Steady-state GTPase assay with membranes of Sf9 cells expressing *hCBR-Gα_{i2}* fusion protein together with Gβ1γ₂ and RGS4, *E*_{max} and logEC₅₀ are presented as mean ± SD, ND: not determined (theoretical value is higher than the highest measured concentration of 100 μM), NT: not tested (compounds are inactive in the screening in *Ag* and *Ant*).

spacer at the imidazole, the bivalent compound **31a** with this spacer at the amide is now an antagonist.

Altogether, the potency of all bivalent ligands decreases to the micromolar range at the *hCB₂R* compared to parent ligand **13a**. But also the standard ligands had shown lower affinities in the functional steady-state GTPase assay³² and for the parent ligand **13a** a 49-fold lower potency than the literature value²⁶ was determined. Therefore, it is reasonable to expect higher affinities for the uni- and bivalent ligands in radioligand binding studies. Nevertheless, at the *hCB₁R* they are potent in the micromolar or higher range. Thus, they largely lose selectivity to the *hCB₂R*, but still show affinity. Due to the coupling with a spacer, the efficacies change and the compounds are no agonists any more. However, the influences of bivalency, spacer length and connecting position are observable. For bivalent ligands with the spacer at the imidazole, bivalency only changes the efficacy at both receptors and has no effect on the potency compared to the corresponding univalent compounds. For the short spacer at the amide, the efficacy at both receptors is changed and the potency is increased due to bivalency. In contrast, for the long spacer at the amide, the bivalency has no influence either on potency or on efficacy. The spacer length leads to a change in the efficacy at both receptors. In addition, also the connecting position has an influence on the efficacy. The bivalent ligands with a short spacer at the imidazole act as antagonists (at the *hCB₂R*) or moderate inverse agonists (at the *hCB₁R*), and with a long spacer as inverse agonist or full inverse agonist, respectively. For bivalent ligands connected at the amide, the short spacer results in inverse agonism (at the *hCB₂R*) or full inverse agonism (at the *hCB₁R*), and the long spacer results in antagonism or moderate inverse agonism, respectively. In the end, a connection of the parent structure with a spacer at the imidazole or at the amide always causes a decrease of potency and a change of efficacy at the *hCB₂R* and *hCB₁R*. This suggests that the receptor–ligand-interactions at both receptors are highly sensitive for changes of the parent structure at both assumed ‘preferred’ attachment positions.

3. Conclusion

In summary, two series of homobivalent ligands with different attachment points containing the parent ligand (*hCB₂R* selective agonist **13a**) and their corresponding univalent ligands were designed and synthesized to target the *hCB₂R*. Biological evaluation of these compounds in a functional steady-state GTPase assay demonstrates that changes of the parent structure at the imidazole or amide have a crucial effect on the potency and efficacy at the *hCB₂R* and *hCB₁R*. They still showed a micromolar activity at both receptors, but no selectivity to the *hCB₂R* and no agonistic behavior. Thus, the receptor–ligand-interaction is very sensitive for changes of the parent structure at these positions. However, it was shown that bivalency had a pronounced influence on the effect of the ligands at the receptors. For bivalent ligands coupled at the imidazole and the bivalent ligand with a short spacer at the amide, bivalency changed the efficacy compared to the univalent compounds. Additionally, for the short bivalent compound **31b** the bivalency was able to increase the potency compared to **26b**. In contrast, for the long spacer at the amide, bivalency did not change potency or efficacy. Furthermore, it was shown that the spacer length and the attachment position also altered the efficacy of these bivalent ligands at the receptors. In addition, the methyl ester **13c** indicates that the ester function at position 5 of the benzimidazole is tolerated with a higher selectivity to the *hCB₂R*, and thus bivalent ligands with an ester coupling might be possible. Further research of bivalent ligands targeting the *hCB₂R*, maybe applying other parent structures, modifying the spacer structure

or linking groups, are needed and may serve as the basis for continuous investigation of the *hCB₂R*. According to these results, very careful design of bivalent ligands for the *hCB₂R* is necessary, especially when agonist properties are planned to be maintained. The results obtained in this study might be of general relevance and interest for the design of bivalent GPCR agonists.

4. Experimental section

4.1. Chemistry

4.1.1. General methods

Unless indicated otherwise, all chemicals and solvents were purchased from commercial suppliers and used without further purification. THF was dried by reflux over sodium overnight and freshly distilled before use. For reactions with dry, freshly distilled THF oven-dried glassware was used. Reactions over argon or nitrogen atmosphere were carried out by filling the reaction apparatuses by a gas flow of the corresponding, commercially available gas and afterwards closing the filled reaction system with a gas-filled balloon. Thin layer chromatography (TLC) was performed on silica gel 60 on aluminum foils with fluorescent indicator 254 nm. For detection iodine vapor and UV light (254 nm and 366 nm) were used. Preparative TLC was performed with silica gel 60 GF₂₅₄ for preparative thin layer chromatography (Merck KGaA). For column chromatography silica gel 60 (particle size: 0.063–0.200 mm or 0.035–0.070 mm) was used. The purity of the target compounds was confirmed by HPLC (degassing unit: DGU20A_{3R}, gradient solvent delivery unit: LC-20AB with two LC-20AD pumps, column: Synergi 4u Fusion-RP 80A 150 × 4.6 mm from Phenomenex Incorporation, UV/vis detector: SPD-20A, analysis software: LabSolutions version 5, everything except the column from Shimadzu Corporation; method parameters: A: H₂O with 0.1% CF₃COOH, B: CH₃OH with 0.1% CF₃COOH, B 10% to 80% 10 min, B 80% 5 min, B 80% to 10% 3 min, flow rate: 1.0 mL min^{−1}, UV detection: 254 nm). The compounds were characterized by a combination of ¹H NMR, ¹³C NMR, mass spectrometry (MS), high resolution MS (HRMS) and elemental analysis. ¹H NMR and ¹³C NMR spectra were recorded on a Bruker AVANCE 300 MHz spectrometer (Bruker BioSpin GmbH) with 300 MHz and 75.5 MHz, respectively or a Bruker AVANCE 400 MHz spectrometer (Bruker BioSpin GmbH) with 400 MHz and 100 MHz, respectively. NMRs were determined in CDCl₃ and chemical shifts are expressed in ppm relative to the solvent peak (¹H NMR: δ 7.26 ppm; ¹³C NMR: δ 77.16 ppm). For MS and HRMS different ionization techniques like ESI, EI or CI were used. MS were performed for ESI with TSQ 7000 (ThermoQuest Finnigan) or Agilent 1100 series LC/MSD ion trap mass spectrometer (Agilent Technologies), for EI and CI with MAT SSQ 710 A (Finnigan). HRMS were measured with Q-TOF 6540 UHD (Agilent Technologies). Elemental analysis for carbon, hydrogen and nitrogen were undertaken using a Vario micro cube (Elementar Analysensysteme GmbH).

4.1.2. General procedure A for amide formation to prepare **8**, **22a–b**, **27a–b**

To a solution of 4-fluoro-3-nitrobenzoic acid (**7**) and a catalytic amount of DMF in CH₂Cl₂ was slowly added a solution of oxalyl dichloride in CH₂Cl₂ at 0 °C. The mixture was stirred at room temperature for 2 h. Then, the solvent was removed in vacuo, some CH₂Cl₂ was added and the solvent was removed again. The brown, oily residue was immediately dissolved in CH₂Cl₂. This solution was slowly added to a solution of the corresponding amine and triethylamine in CH₂Cl₂ at 0 °C. The mixture was stirred overnight at room temperature. After removal of solvent in vacuo the crude product was dispersed in concentrated Na₂CO₃ solution, and

extracted with CH_2Cl_2 . The combined organic phases were dried over anhydrous Na_2SO_4 . After filtration and removal of solvent in vacuo the product was purified by column chromatography to yield the corresponding amide.

4.1.3. General procedure B for the substitution of fluoride to prepare 10a–c, 14a–b, 18a–c, 23a–b, 28a–b

The corresponding amine and triethylamine were dissolved in ethanol and stirred at room temperature for 0.5–1 h. Then, a solution of the corresponding 4-fluoro-3-nitrophenyl compound in ethanol was slowly added. The mixture was stirred overnight at 50–75 °C. After removal of solvent in vacuo the product was purified by column chromatography to give the corresponding 4-amino-3-nitrophenyl compound.

4.1.4. General procedure C for the reduction of the nitro group by stannous chloride to prepare 11a–b, 19a–c, 29a–b

The corresponding 4-amino-3-nitrophenyl compound was dissolved in ethanol and $\text{SnCl}_2 \cdot 2\text{H}_2\text{O}$ was added. The mixture was stirred overnight at 75 °C under argon atmosphere. After cooling at 0 °C the mixture was basified with concentrated NaOH solution (pH >10) and filtered by suction. Then, the solution was concentrated in vacuo. The residue was dispersed in water and extracted with CH_2Cl_2 . The combined organic phases were dried over anhydrous Na_2SO_4 . After filtration the solvent was removed in vacuo to give the corresponding crude 3,4-diaminophenyl compound, which was immediately used in the next step.

4.1.5. General procedure D for the reduction of the nitro group by iron powder to prepare 11c, 15a–b, 24a–b

The corresponding 4-amino-3-nitrophenyl compound was dissolved in ethanol and water. Iron powder and 37% (w/w) HCl solution was added. The mixture was stirred at reflux for 2 h under argon or nitrogen atmosphere. After cooling the mixture was basified with 25% (w/w) NH_3 solution (pH ~9–10) and filtrated by suction. Then, the solution was concentrated in vacuo. The residue was dispersed in water, once more basified with 25% (w/w) NH_3 solution (pH ~9–10) and extracted with ethyl acetate or CH_2Cl_2 . The combined organic phases were dried over anhydrous Na_2SO_4 . After filtration the solvent was removed in vacuo to give the corresponding crude 3,4-diaminophenyl compound, which was immediately used in the next step.

4.1.6. General procedure E for amide formation to prepare 12a–c, 16a–b, 20a–c, 25a–b, 30a–b

2-(4-Ethoxyphenyl)acetic acid and CDI were dissolved in dry, freshly distilled THF and stirred at room temperature for 2 h. Then, a solution of the corresponding 3,4-diaminophenyl compound in dry, freshly distilled THF was added. The mixture was stirred overnight at 50 °C under argon or nitrogen atmosphere. After removal of solvent in vacuo the residue was dispersed in water and extracted with ethyl acetate or CH_2Cl_2 . The combined organic phases were dried over anhydrous Na_2SO_4 . After filtration and removal of solvent in vacuo the product was purified by column chromatography to yield the corresponding amide.

4.1.7. General procedure F for the ring-closure to prepare 13a–c, 17a–b, 21a–c, 26a–b, 31a–b

The corresponding amide was dissolved in glacial acetic acid and stirred at reflux for 1.5–3 h. After concentrating in vacuo the residue was slowly dispersed in 1 M NH_3 solution (pH ~9–10) and extracted with ethyl acetate or CH_2Cl_2 . The combined organic phases were dried over anhydrous Na_2SO_4 . After filtration and removal of solvent in vacuo the product was purified by column chromatography or preparative TLC to yield the corresponding benzimidazole. For elemental analysis the hydrochlorides of 13a–b, 21b–c, 31b were prepared by dissolving of the compounds in a diethyl ether/ CH_2Cl_2 mixture, and precipitation of the salts with 2 M HCl in diethyl ether. After filtration by suction and drying in vacuo the corresponding hydrochlorides were obtained.

4.2. Pharmacology

4.2.1. Functional steady-state GTPase assay

4.2.1.1. Materials. The standard ligands (Fig. 5) CP 55,940, AM 251, AM 630 and SR 144,528 were purchased either from Tocris Cookson (Bristol, UK) or Santa Cruz Biotechnology (Dallas, TX, USA). DMSO was from Merck (Darmstadt, Germany). Tris(hydroxymethyl)aminomethane (Tris) was bought from USB (Cleveland, OH, USA). Adenosine 5'-triphosphate (ATP), guanosine 5'-triphosphate (GTP), adenosine 5'-(β , γ -imido)triphosphate (AppNHP), creatine kinase (CK), creatine phosphate (CP), bovine serum albumin (BSA), ethylenediaminetetraacetic acid (EDTA), activated charcoal and salts were purchased either from Roche Diagnostics (Mannheim, Germany) or Sigma–Aldrich (St. Louis, MO, USA). The scintillation cocktail OptiPhase Supermix was acquired from PerkinElmer (Waltham, MA, USA). The [γ - ^{33}P]GTP was bought from Hartmann Analytic (Braunschweig, Germany). Radioactive samples were counted in a Tricarb-TR liquid scintillation analyzer from PerkinElmer (Waltham, MA, USA).

4.2.1.2. Assay. Stock solutions of all compounds were prepared in DMSO and stored at –20 °C. Dilutions were prepared with 30% (v/v) DMSO and also stored at –20 °C. Final DMSO concentrations in assay tubes were always 3% (v/v) and did not affect the assay.

Steady-state GTPase assay was performed as previously described:³² Reaction tubes contained 100 μL of membrane (5 μg protein/tube) of Sf9 cells expressing either $h\text{CB}_2\text{R}-\text{G}\alpha_{i2}$ or $h\text{CB}_1\text{R}-\text{G}\alpha_{i2}$ fusion protein together with $\text{G}\beta_1\gamma_2$ and RGS4,³³ 0.1 mM ATP, 0.1 μM GTP, 0.1 mM AppNHP, 1 μg CK, 30 μg CP, 0.2% (w/v) BSA, 0.1 mM EDTA, 1 mM MgCl_2 , various concentrations of test compounds and 0.05 $\mu\text{Ci}/\text{mL}$ [γ - ^{33}P]GTP in 50 mM Tris/HCl pH 7.4. Reactions were conducted at 25 °C for 20 min, stopped by addition of 900 μL of 50 mM sodium phosphate buffer pH 2.0 containing 5% (w/v) activated charcoal and centrifuged at 12,000 rpm to remove not degraded [γ - ^{33}P]GTP. 600 μL of supernatant fluid was used and radioactivity in counts per minute was determined in 3 mL of scintillation cocktail. Spontaneous degradation of

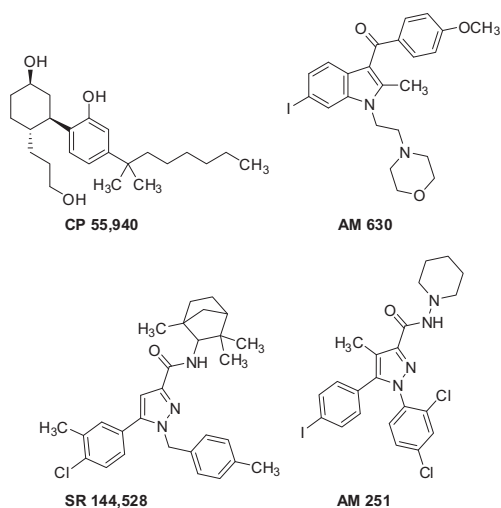


Figure 5. Structures of $h\text{CB}_2\text{R}$ and $h\text{CB}_1\text{R}$ unselective agonist CP 55,940, $h\text{CB}_2\text{R}$ selective antagonist AM 630, $h\text{CB}_2\text{R}$ selective inverse agonist SR 144,528 and $h\text{CB}_1\text{R}$ selective inverse agonist AM 251.^{3,36–39}

[γ - ^{33}P]GTP was determined by adding 1 mM unlabeled GTP and enzyme activity was corrected for spontaneous degradation.

Basal GTPase activities were determined only with a final concentration of 3% (v/v) DMSO instead of ligand dilutions and set as 0% value for screening. GTPase activity increase of 30 μM of CP 55,940 was set as 100% in agonism mode (Ag) and 30 nM of CP 55,940 was set as 100% in antagonism mode (Ant). Screening of ligands was performed with compound concentrations of 30 μM , without additional CP 55,940 in Ag and in presence of 30 nM CP 55,940 in Ant.

Dose–response curves were conducted with at least 5 different concentrations from 0.1 nM to 100 μM in the appropriate mode determined in the previous screening.

4.2.1.3. Statistical analysis. Statistical evaluations and sigmoidal dose–response curve fittings were performed with GraphPad Prism 5 software for Windows (La Jolla, CA, USA). Data are expressed as mean values \pm standard deviations (SD) of three independent experiments with three different batches of membranes each performed in duplicates or triplicates. Statistical significance was determined by one-way ANOVA followed by Dunnett's post test.

Acknowledgment

M. Decker gratefully acknowledges the German Research Foundation (DFG) for financial support (DFG DE 1546/4-1).

Appreciation is expressed to Professor S. Elz for supporting the synthesis in his chemical laboratories, and to M. Beer-Krön, M. Flemming and S. Pockes for support in performance of the steady-state GTPase assay.

Supplementary data

Supplementary data associated with this article can be found, in the online version, at <http://dx.doi.org/10.1016/j.bmc.2014.06.008>.

References and notes

- Gaoni, Y.; Mechoulam, R. *J. Am. Chem. Soc.* **1964**, *86*, 1646.
- Mechoulam, R.; Gaoni, Y. *J. Am. Chem. Soc.* **1965**, *87*, 3273.
- Howlett, A. C.; Barth, F.; Bonner, T. I.; Cabral, G.; Casellas, P.; Devane, W. A.; Felder, C. C.; Herkenham, M.; Mackie, K.; Martin, B. R.; Mechoulam, R.; Pertwee, R. G. *Pharmacol. Rev.* **2002**, *54*, 161.
- de Fonseca, F. R.; del Arco, I.; Bermudez-Silva, F. J.; Bilbao, A.; Cippitelli, A.; Navarro, M. *Alcohol Alcohol.* **2005**, *40*, 2.
- de Petrocellis, L.; di Marzo, V. *Best Pract. Res. Clin. Endocrinol.* **2009**, *23*, 1.
- Console-Bram, L.; Marcu, J.; Abood, M. E. *Prog. Neuro-Psychopharmacol.* **2012**, *38*, 4.
- Hiller, C.; Kühhorn, J.; Gmeiner, P. *J. Med. Chem.* **2013**, *56*, 6542.
- Shonberg, J.; Scammells, P. J.; Capuano, B. *ChemMedChem* **2011**, *6*, 963.
- Mohr, K.; Schmitz, J.; Schrage, R.; Tränkle, C.; Holzgrabe, U. *Angew. Chem., Int. Ed.* **2013**, *52*, 508.
- Lane, L. R.; Sexton, P. M.; Christopoulos, A. *Trends Pharmacol. Sci.* **2013**, *34*, 59.
- Portoghese, P. S.; Larson, D. L.; Sayre, L. M.; Yim, C. B.; Ronsisvalle, G.; Tam, S. W.; Takemori, A. E. *J. Med. Chem.* **1986**, *29*, 1855.
- Decker, M.; Fulton, B. S.; Zhang, B.; Knapp, B. I.; Bidlack, J. M.; Neumeyer, J. L. *J. Med. Chem.* **2009**, *52*, 7389.
- Decker, M.; Si, Y.-G.; Knapp, B. I.; Bidlack, J. M.; Neumeyer, J. L. *J. Med. Chem.* **2010**, *53*, 402.
- Zhang, B.; Zhang, T.; Sromek, A. W.; Scrimale, T.; Bidlack, J. M.; Neumeyer, J. L. *Bioorg. Med. Chem.* **2011**, *19*, 2808.
- Abadi, A. H.; Lankow, S.; Hoefgen, B.; Decker, M.; Kassack, M. U.; Lehmann, J. *Arch. Pharm. (Weinheim)* **2002**, *335*, 367.
- Decker, M.; Lehmann, J. *Curr. Top. Med. Chem.* **2007**, *7*, 347.
- Kühhorn, J.; Hübner, H.; Gmeiner, P. *J. Med. Chem.* **2011**, *54*, 4896.
- Gogoi, S.; Biswas, S.; Modi, G.; Antonio, T.; Reith, M. E. A.; Dutta, A. K. *ACS Med. Chem. Lett.* **2012**, *3*, 991.
- Huber, D.; Löber, S.; Hübner, H.; Gmeiner, P. *Bioorg. Med. Chem.* **2012**, *20*, 455.
- Vermaak, J. C.; de Kock, M. A.; Joubert, J. R. S. *Afr. Med. J.* **1972**, *46*, 1999.
- Jacobsen, J. R.; Choi, S. K.; Combs, J.; Fournier, E. J. L.; Klein, U.; Pfeiffer, J. W.; Thomas, G. R.; Yu, C.; Moran, E. J. *Bioorg. Med. Chem. Lett.* **2012**, *22*, 1213.
- Eiden, F.; Gerstlauer, C. *Arch. Pharm. (Weinheim)* **1981**, *314*, 995.
- Zhang, Y.; Gilliam, A.; Maitra, R.; Damaj, M. I.; Tajuba, J. M.; Seltzman, H. H.; Thomas, B. F. *J. Med. Chem.* **2010**, *53*, 7048.
- Fernández-Fernández, C.; Decara, J.; Bermúdez-Silva, F. J.; Sánchez, E.; Morales, P.; Gómez-Cañas, M.; Gómez-Ruiz, M.; Callado, L. F.; Goya, P.; de Fonseca, F. R.; Martín, M. I.; Fernández-Ruiz, J.; Meana, J. J.; Jagerovic, N. *Arch. Pharm. Chem. Life Sci.* **2013**, *346*, 171.
- Naour, M. L.; Akgün, E.; Yekkirala, A.; Lunzer, M. M.; Powers, M. D.; Kalyuzhny, A. E.; Portoghese, P. S. *J. Med. Chem.* **2013**, *56*, 5505.
- Pagé, D.; Balaux, E.; Boisvert, L.; Liu, Z.; Milburn, C.; Tremblay, M.; Wei, Z.; Woo, S.; Luo, X.; Cheng, Y.-X.; Yang, H.; Srivastava, S.; Zhou, F.; Brown, W.; Tomaszewski, M.; Walpole, C.; Hodzic, L.; St-Onge, S.; Godbout, C.; Salois, D.; Payza, K. *Bioorg. Med. Chem. Lett.* **2008**, *18*, 3695.
- Pagé, D.; Brochu, M.-C.; Yang, H.; Brown, W.; St-Onge, S.; Martin, E.; Salois, D. *Lett. Drug Des. Discovery* **2006**, *3*, 298.
- Verbist, B. M. P.; De Cleyne, M. A. J.; Surkyn, M.; Fraiponts, E.; Aerssens, J.; Nijssen, M. J. M. A.; Gijzen, H. J. M. *Bioorg. Med. Chem. Lett.* **2008**, *18*, 2574.
- Gijzen, H. J. M.; De Cleyne, M. A. J.; Surkyn, M.; Van Lommen, G. R. E.; Verbist, B. M. P.; Nijssen, M. J. M. A.; Meert, T.; Van Wauwe, J.; Aerssens, J. *Bioorg. Med. Chem. Lett.* **2012**, *22*, 547.
- Watson, C.; Owen, D. R.; Harding, D.; Kon-I, K.; Lewis, M. L.; Mason, H. J.; Matsumizu, M.; Mukaiyama, T.; Rodriguez-Lens, M.; Shima, A.; Takeuchi, M.; Tran, I.; Young, T. *Bioorg. Med. Chem. Lett.* **2011**, *21*, 4284.
- Pagé, D.; Wei, Z.; Liu, Z.; Tremblay, M.; Desfossés, H.; Milburn, C.; Srivastava, S.; Yang, H.; Brown, W.; Walpole, C.; Tomaszewski, M.; St-Onge, S.; Lessard, E.; Payza, K.; Panetta, R.; Yu, X. H.; Groblewski, T. *Lett. Drug Des. Discovery* **2010**, *7*, 208.
- Geiger, S.; Nickl, K.; Schneider, E. H.; Seifert, R.; Heilmann, J. *Naunyn-Schmiedeberg's Arch. Pharmacol.* **2010**, *382*, 177.
- Sutor, S.; Heilmann, J.; Seifert, R. *J. Pharm. Pharmacol.* **2011**, *63*, 1043.
- Sutor, S. (Ph.D. Dissertation), Universität Regensburg, 2010.
- Seifert, R.; Wenzel-Seifert, K. *Life Sci.* **2003**, *73*, 2263.
- Pertwee, R.; Griffin, G.; Fernando, S.; Li, X.; Hill, A.; Makriyannis, A. *Life Sci.* **1995**, *56*, 1949.
- Portier, M.; Rinaldi-Carmona, M.; Pecceu, F.; Combes, T.; Poinot-Chazel, C.; Calandra, B.; Barth, F.; le Fur, G.; Casellas, P. *J. Pharmacol. Exp. Ther.* **1999**, *288*, 582.
- Pertwee, R. G. *Int. J. Obes.* **2006**, *30*, S13.
- Pertwee, R. G. *Life Sci.* **2005**, *76*, 1307.